

# Supplemental Material for “Secondary Fast Breakdown in Narrow Bipolar Events”

Dongshuai Li<sup>1</sup>, Alejandro Luque<sup>1</sup>, F. J. Gordillo-Vázquez<sup>1</sup>, Caitano da Silva<sup>2</sup>, Paul R. Krehbiel<sup>2</sup>, Farhad Rachidi<sup>3</sup>, Marcos Rubinstein<sup>4</sup>

<sup>1</sup>Instituto de Astrofísica de Andalucía (IAA), CSIC, Granada, Spain.

<sup>2</sup>Langmuir Laboratory for Atmospheric Research, New Mexico Institute of Mining and Technology, Socorro, USA.

<sup>3</sup>Electromagnetic Compatibility Laboratory, Swiss Federal Institute of Technology (EPFL), Lausanne, Switzerland.

<sup>4</sup>University of Applied Sciences and Arts Western Switzerland, Yverdon-les-Bains, Switzerland.

## Contents of this file

1. Text S1 and S2
2. Figures S1 - S5

### **Text S1: The effect of adding an extra region where the current decays smoothly**

We present here an extension of the Modified Transmission Line with Exponential decay (MTLE) model by adding an extra region where the current decays smoothly. As shown in Figure S2, we assume the steamer coronas interact with the negative charges and disappear naturally within the added region with a length of  $d$ . From the altitude  $H_2$

---

to  $H_1$  with a length of  $L$ , the current distribution is still based on the MTLE model, with a current  $I(z, t)$  that propagates downward and decreases exponentially along its propagation channel with the attenuation rate  $\lambda$ :

$$I(z, t) = I \left( t - \frac{H_2 - z}{v} \right) e^{(H_2 - z)/\lambda}, \quad (H_1 < z < H_2) \quad (1)$$

where  $v$  is the propagation velocity. Then we add an extra region with a length of  $d$  below  $H_1$  where the current decays linearly:

$$I(z, t) = I \left( t - \frac{H_2 - z}{v} \right) e^{(H_2 - H_1)/\lambda} \left( 1 - \frac{H_1 - z}{d} \right), \quad (H_1 - d < z < H_1) \quad (2)$$

The results of adding this extra region are presented in Figure S3. We use Uman's equation with the same current parameters adopted by Rison et al. (2016). For both NBE1 and NBE3, the calculated results disagree with the measurements. Moreover, an unrealistically long extension with  $d \geq 5$  km is required to sufficiently attenuate the radiated field peaks for both NBE1 and NBE3.

### **Text S2: The results corresponding to the bouncing-wave model**

The bouncing-wave model proposed by Nag & Rakov (2010) assumes that the NBE current propagates uniformly along a conducting transmission line (TL) channel and is reflected multiple times at either end of the channel. As shown in Figure S4, the downward current pulse hits the bottom of the channel where it is reflected and begins traveling upward. In general, the pulse will experience multiple reflections at the top and bottom of the channel with losses accounted for by the current reflection coefficients  $\rho_t$  and  $\rho_b$ , respectively.

The downward current  $I_d(z, t)$  is given by

$$I_d^n(z, t) = \sum_{n=1,3,5,\dots}^{\infty} \rho_b^{\frac{n-1}{2}} \rho_t^{\frac{n-1}{2}} I_0 \left( z, t - \frac{(n-1)(H_2 - z)}{v} \right), \quad (3)$$

where  $I_0$  is the incident current. Similarly, the upward current  $I_u(z, t)$  is

$$I_u^n(z, t) = \sum_{n=2,4,6,\dots}^{\infty} \rho_b^{\frac{n}{2}} \rho_t^{\frac{n}{2}-1} I_0 \left( z, t - \frac{(n-1)(H_2 - z)}{v} \right). \quad (4)$$

Then, the total current  $I_{total}(z, t)$  is obtained as

$$I_{total}(z, t) = \sum_{n=1,3,5,\dots}^{\infty} I_d^n(z, t) + \sum_{n=2,4,6,\dots}^{\infty} I_u^n(z, t) \quad (5)$$

In Figure S5 we show the results corresponding to the bouncing-wave model by considering different current reflection coefficients for both NBE1 and NB3. The incident current  $I_0$  and its parameters are considered the same as those adopted in Rison et al. (2016). Here, we present four cases where  $\rho_b = \rho_t = 0$  (the current wave is fully absorbed at both top and bottom ends),  $\rho_b = \rho_t = 1$  (the same current wave bounding at both top and bottom ends),  $\rho_b = \rho_t = -1$  (the current wave changes polarity at both top and bottom ends ) and  $\rho_b = \rho_t = -0.5$  (the current wave changes polarity and is partially absorbed to reduce its magnitude to be half at both the top and bottom ends).

In their original bouncing-wave proposal, Nag & Rakov (2010) explained the secondary pulse as the reflection of a wave as it reaches the end of an established conductor channel. However, observations of thunderstorm activity have shown that there is no evidence of a leader channel being established before the NBEs (Rison et al., 2016). Moreover, it can be seen from Figure S5 that the calculated results using the bouncing-wave model can not match well with the measurements.

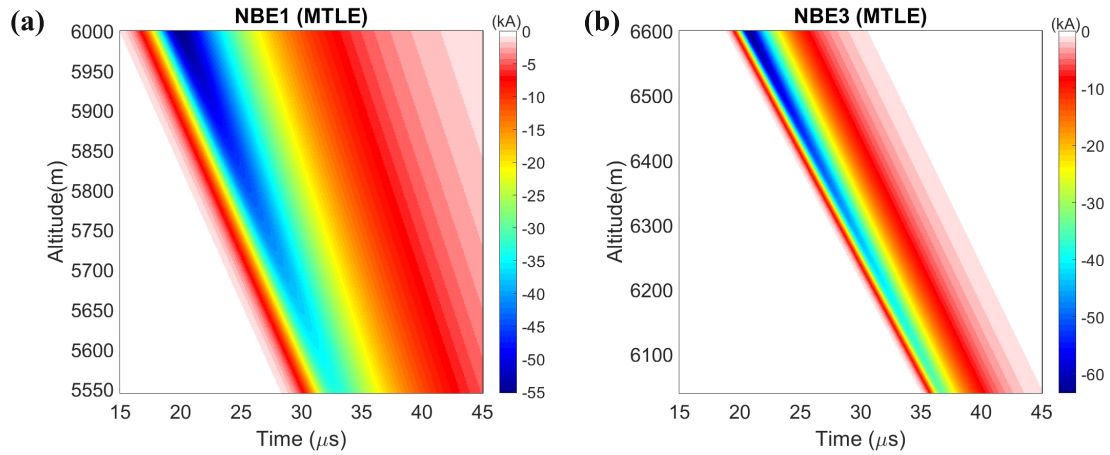


**Figure S1.** The current distribution as a function of height for the MTLE model corresponding to the cases NBE1 (a) and NBE3 (b) in Rison et al. (2016). The adopted parameters are the same as those used by Rison et al. (2016), which are also presented in table 1.

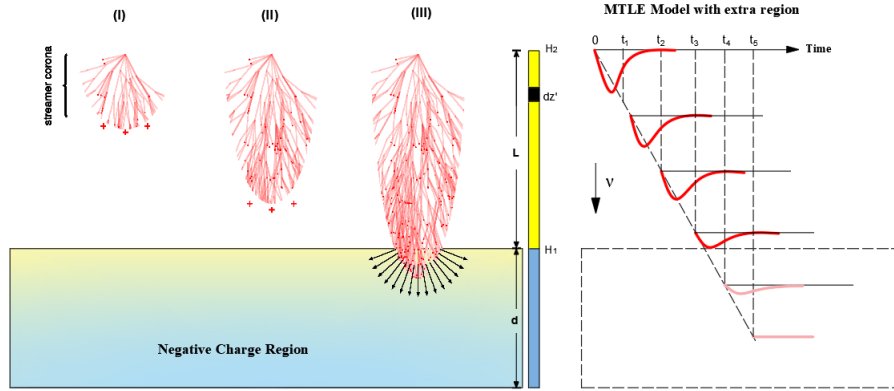


**Figure S2.** The MTLE model with an extra region ( $d$ ) where the current decays smoothly, (I)-(III) are different growth stages of the steamer corona system of NBEs. In the extra region, the steamer coronas are assumed to interact with the negative charges and disappear naturally.

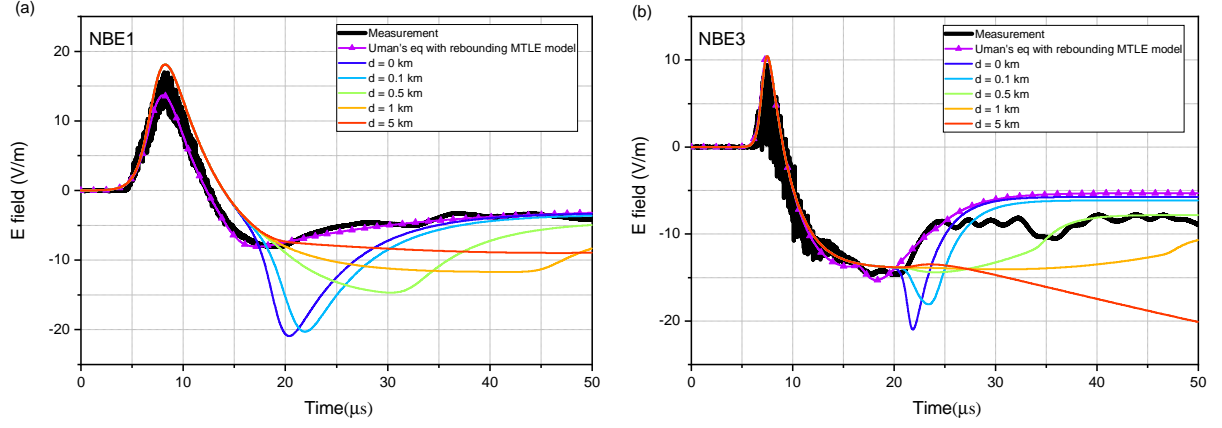


**Figure S3.** Comparison between simulation and measurement corresponding to the case NBE1 (a) and NBE3 (b) in Rison et al. (2016). The simulation is based on Uman's equation with  $d$  ranging from 0 km to 5 km. The results from the rebounding MTLE model are also presented in the figure.

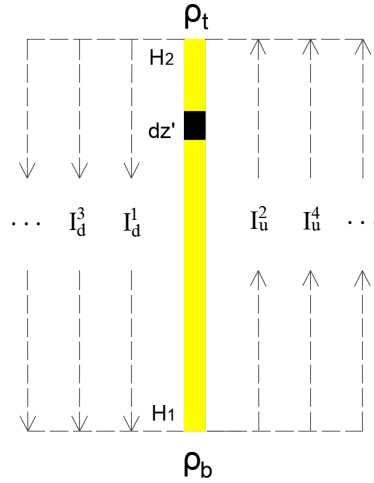


**Figure S4.** The bouncing-wave model proposed by Nag & Rakov (2010). The NBE current propagates downwards from an altitude  $H_2$  to  $H_1$  with a channel length  $L$ . Inside the conducting channel, the current will experience multiple reflections at the top and bottom ends with the current reflection coefficients  $\rho_t$  and  $\rho_b$ , respectively.  $I_d^n$  and  $I_u^n$  are the downward and upward currents at the  $n$ th reflection.

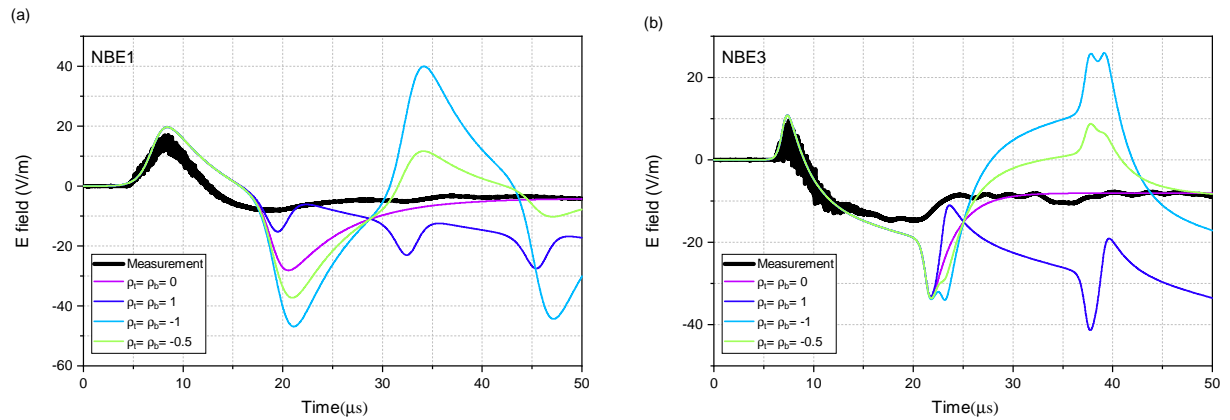


**Figure S5.** Comparison between simulation and measurement corresponding to the cases NBE1 (a) and NBE3 (b) in Rison et al. (2016). The simulation is based on the bouncing-wave model (Nag & Rakov, 2010) adopting different sets of the current reflection coefficients as indicated in the figure legend.

## References

- Nag, A., & Rakov, V. A. (2010). Compact intracloud lightning discharges: 1. Mechanism of electromagnetic radiation and modeling. *Journal of Geophysical Research: Atmospheres*, *115*(D20). doi: 10.1029/2010JD014235
- Rison, W., Krehbiel, P. R., Stock, M. G., Edens, H. E., Shao, X.-M., Thomas, R. J., ... Zhang, Y. (2016). Observations of narrow bipolar events reveal how lightning is initiated in thunderstorms. *Nature communications*, *7*, 10721. doi: 10.1038/ncomms10721(2016)